Flat multi-core fibre for twist elimination in distributed bend sensing

Angeliki Zafeiropoulou[a,b,*], Ali Masoudi[b], Laurence Cooper[a], Gilberto Brambilla[b]

[a] *Fibercore House, Science Park, University Parkway, Chilworth, Southampton SO16 7QQ*
[b] *Optoelectronics Research Centre, University of Southampton, Southampton SO17 1BJ*

Abstract

Optical fibre sensors offer many advantages in comparison to their conventional counterparts, such as extremely low sensitivity to external electromagnetic fields and small dimensions. The multi-core fibres in particular are ideal candidates for shape sensing due to the intrinsic 3D coordinate system they offer. However the twist of the multi-core fibre during its deployment along the structure of interest, distorts the 3D coordinate system based on their fixed position. In this work a multi-core fibre of unique geometry is presented as a solution to this issue. Owing to its two flat sides, this fibre presents enhanced preferential bending that eliminates the random twist of the sensing fibre.

1. Introduction

Multi-core fibres (MCF) were first exploited as a way to increase the data-carrying capacity of a single optical fibre [1]. MCF contain multiple cores in the same cladding allowing for parallel paths resulting in an increase in the bandwidth capacity through space division multiplexing. Over the last few years MCF have attracted significant attention in optical fibre sensing when used in conjunction with Fibre Bragg Gratings (FBGs) [2], [3], [4], [5], or with distributed techniques based on Rayleigh scattering such as Optical Frequency

*Fully documented templates are available in the elsarticle package on CTAN.
*Corresponding author
Email address: azafeiropoulou@fibercore.com (Angeliki Zafeiropoulou)

Domain Reflectometry (OFDR) [6], [7] or a combination of Brillouin Optical Time-Domain Analysis (B-OTDA) and Rayleigh phase Optical Time-Domain Reflectometry (ϕ-OTDR) [8].

MCF are very good candidates for shape sensing applications [9] due to the intrinsic 3D-coordinate system they offer owing to the fixed position of the cores within the cladding [10], [11]. However a common challenge when using multi-core fibres is the twist of the fibre as it is being deployed along the structure of interest. Twist is a torsion along the fibre longitudinal axis. This results in a subsequent twist of the cores, distorting the 3D coordinate system needed for shape sensing introducing large errors in the curvature. It additionally causes uncertainty in the determination of the bending direction [12].

Previous attempts of addressing this issue include the use of a spun multi-core fibre with FBGs inscribed in it to increase the twist sensitivity and hence measure the undesired twist [12], [13]. Once the twist is measured a numerical method is used in the signal processing stage, to compensate for this twist [14]. Despite the high sensitivity and accuracy achieved with the proposed method, the need for compensation increases the complexity of the post processing introducing a potential error [15]. In addition, a spun multi-core fibre is required which has a more challenging fabrication process compared to that of an unspun multi-core [16]. This is because the spun fibre has to be drawn at a low temperature and high tension, which causes fibre breakages during the draw. An alternative way of addressing the twist issue was reported by Zhao et al. who used a standard 7CF and a BOTDA setup for curvature measurements [10]. To prevent the fibre from twisting, they used an optical microscope to manually orient the fibre hence maintaining the relative position of the cores with respect to the bending plane. However, this approach cannot be easily implemented in the field, especially over a long sensing range.

In a recent work by Zafeiropoulou et al. [17] an alternative method for addressing the issue of twist was explored that was based solely on the mechanical properties of the fibre. In the aforementioned work a multi-core fibre with one flat side (a D-shaped multi-core fibre) was designed and fabricated to enhance

the bending preference of the fibre. Thanks to its unique geometry, the said fibre bends preferentially along a plane that is parallel to its flat side. Although the D-shaped side maintains the same orientation along the fibre for a longer length compared to a standard 7CF, however it still flips between two possible states as stress is built on one side while the fibre is being wrapped around the spool: Either the flat side faces the inner side of the spool or the outside.

In the current study, an improved multi-core fibre design is presented that addresses the flips and greatly enhances the preference in bending, leading to a fibre that self-aligns itself in a way that the twist is eradicated. The flat multi-core fibre presents a strong resistance to bending, owing to its distinctive geometry that consists of two flat sides. The use of this fibre completely eradicates the twist, eliminating the need for numerical compensation, rendering this multi-core fibre the perfect candidate for shape sensing applications. In addition to its inherent ability to maintain its orientation along the fibre length, its rectangular coating contributes to an easy identification of the flat sides, simplifying the deployment of this fibre along the structure of interest.

2. Principle of distributed sensing using Brillouin scattering

Brillouin scattering is an inelastic scattering process associated to the acoustic phonons of a material. The frequency shifts associated to this process are given by [18],

$$f_B = \frac{2n_{\text{core}}V_a}{\lambda} \tag{1}$$

where n_{core} is the core refractive index, V_a is the velocity of sound and λ is the vacuum wavelength. Eq. 1 shows that the Brillouin frequency shift depends upon the acoustic velocity in the fibre (which in turn depends on the Young's modulus E of the material, the Poisson ratio μ and the density ρ [19]) as well as the fibre refractive index. Since all the above parameters are temperature and strain dependent, the frequency shift provides information about the strain and temperature that caused it.

Sensing systems based on Brillouin scattering can be used for long range sensing such as for structural health monitoring of civil structures [20]. In applications like these it is highly desirable to monitor the shape of the structure, gaining information in advance to prevent catastrophic events. Shape sensing with optical fibres, refers to the reconstruction of the shape of an object using the strain that has been induced to the fibre by the bend [21]. The sensing principle using multi-core fibres is described below: When the cores experience no tension then the measured frequency shift from each core of the multi-core fibre is uniform along the length of the fibre. When the fibre is bent, some of the cores experience tension while others experience compression, depending on their relative position with respect to the neutral axis. As a result of this, the elongation of the cores leads to a frequency upshift while the compressed cores experience a downshift in frequency. By measuring the frequency shift Δf_{Bi} of core-i, the strain at core-i, ϵ_i, can be calculated according to the following linear relationship:

$$\frac{\Delta f_{Bi}}{f_B} = C_\epsilon \epsilon_i \tag{2}$$

where C_ϵ is the strain coefficient and f_B is the initial BFS in a reference condition. Using the strain information, the radius of curvature and the direction of bending can be calculated using various shape sensing algorithms [21], [22].

In the current study, the frequency shifts were measured using Brillouin-OTDR, a single-ended technique in which a pulse of laser is sent down the sensing fibre and the intensity of the spontaneous Brillouin scattering is used to map the temperature and strain along the fibre [23].

3. Experimental arrangement

3.1. Brillouin OTDR setup

Fig. 1 shows a schematic diagram of the experimental setup. Light from a Tunable Laser Source (TLS) at 1533nm was amplified by an Erbium-Doped

Fibre Amplifier (EDFA 1) and then split by a 70/30 coupler. Light from the 70% arm of the coupler was amplitude-modulated using an Electro-Optic Modulator (EOM) to generate a train of 10ns pulses with a repetition rate of 1MHz. The light was further amplified by another optical amplifier (EDFA 2) before entering an Acousto-Optic Modulator (AOM), which limits the Amplified Spontaneous Emission (ASE) entering the sensing fibre. The AOM was synchronised with the EOM to allow the probe pulse to pass through.

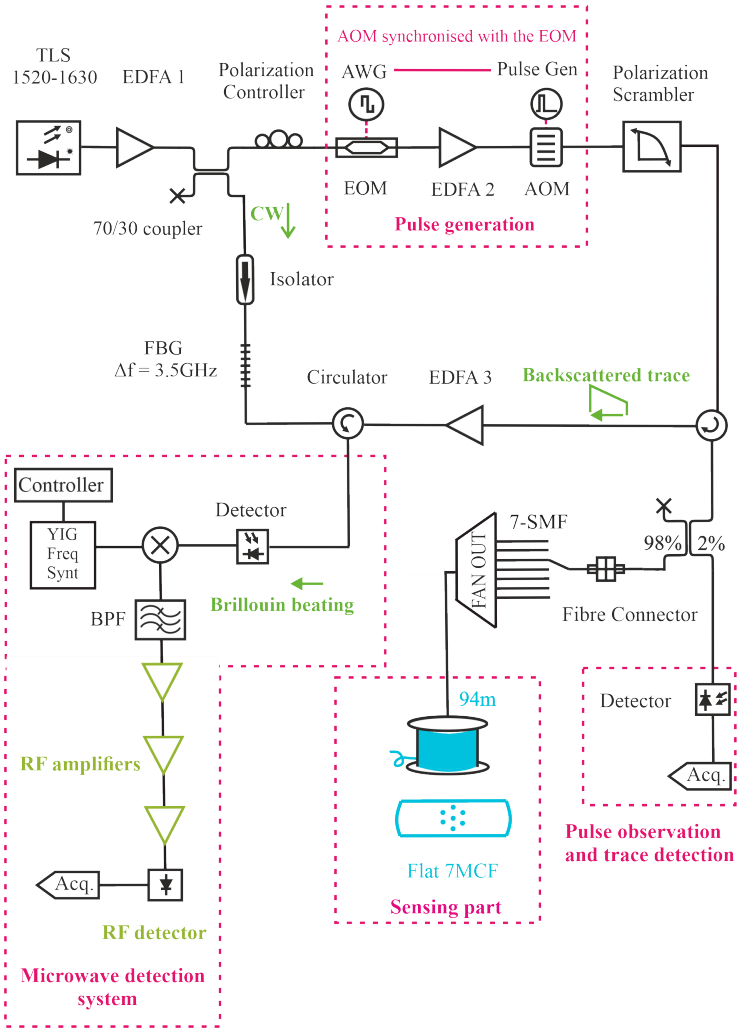

Figure 1: Experimental Setup. TLS, Tunable Laser Source; AWG, Arbitrary Wave Function; EOM, Electro-Optic Modulator; EDFA, Erbium-Doped Fibre Amplifier; AOM, Acousto-Optic Modulator; BPF, Band Pass Filtre; YIG, Yttrium Iron Garnet Frequency Synthesiser; YIG Freq Synt.

100 A polarisation scrambler was added in order to avoid polarisation fading. The amplified probe pulse with a peak power of 1 W was then launched into the sensing fibre via a circulator. A 98/2 tap coupler was added after the second port of the circulator to monitor the probe pulse. The remaining 98% of the

power was sent to the sensing fibre via a fan-out demultiplexer. A 94m long, flat 7CF was spliced to a custom made flat MCF fan-out [24]. The backscattered light from the sensing fibre was amplified by a third optical amplifier (EDFA 3) followed by a narrow bandwidth FBG (λ_B = 1533.35 nm, BW = 3.5 GHz to separate the Brillouin anti-Stokes from the Rayleigh backscattering. The Brillouin backscattered trace was mixed with the seed laser from the 30% arm of the 30/70 coupler. The 10.5 GHz beat signal generated corresponding to the Brillouin frequency shift was detected using a 15 GHz photodetector with a responsivity greater than 0.95 A/W at 1550 nm. The frequency of the signal was further down-shifted using a microwave detection system. More specifically the backscattered signal from the sensing fibre was mixed with the signal generated by an Yttrium Iron Garnet (YIG) frequency synthesiser. After mixing, the signal was passed through a Band-Pass Filter (BPF) centred at 1 GHz, with a bandwidth of 50 MHz to generate an Intermediate Frequency (IF) of 1 GHz. The IF signal was amplified by two stage RF amplifier and then rectified using a microwave diode rectifier generating a signal proportional to the intensity of the Brillouin backscattering at the chosen frequency. An oven controlled crystal oscillator was used to provide the YIG synthesiser with a stable reference frequency [25].

3.2. Fabrication process of the flat fibre.

The fabrication of the flat fibre started with the Multi-Core (MC) preform assembly. The cladding preform has been fabricated using the slurry-casting method [26]. The solid MCF preform was then stretched to a 3 : 1 ratio, inserted into a sleeving tube and then sleeved before the milling. The core preforms, that were fabricated using MCVD [27], had an extra large size and were then stretched and divided into 7 rods which were inserted into the preform holes. As a final step of the preform fabrication, the 35 mm in diameter preform was mounted on a milling bed and a diamond milling tool was used to mill both sides by 5.9 mm. The fabrication stages of the flat preform as well as the dimensions of the preforms are depicted in Fig. 2.

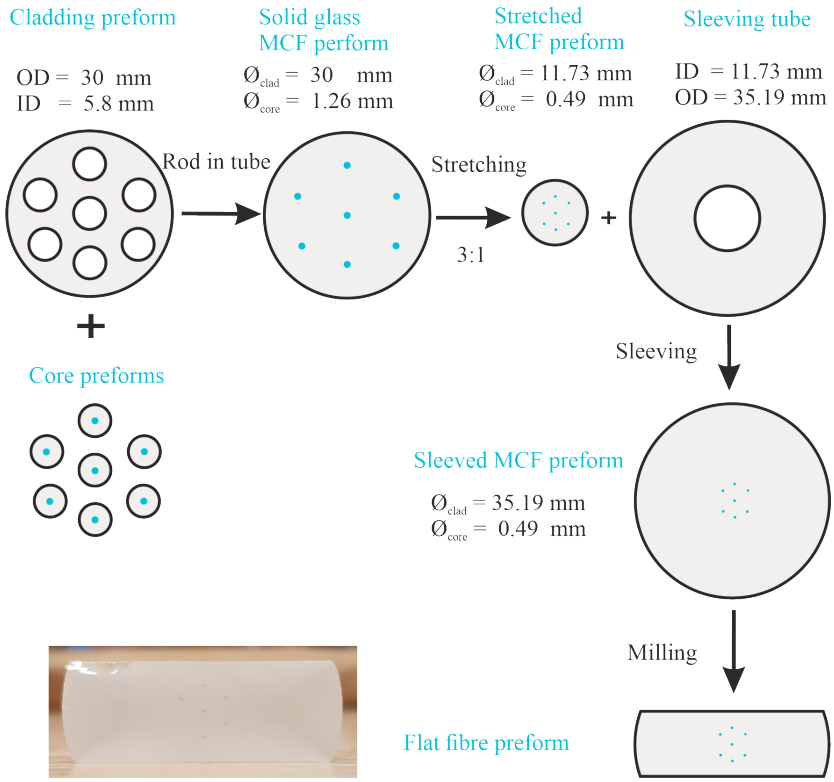

Figure 2: Core preforms that were fabricated using MCVD were inserted in the cladding preform fabricated by the slurry casting method. The 7CF preform that was produced after the sealing process was then stretched to a 3:1 ratio in order to fit into the sleeving tube. After sealing, the sleeved MCF was milled to the desired size. The fibre cross-section as well as a microscope picture of the rectangular split dies, are also shown.

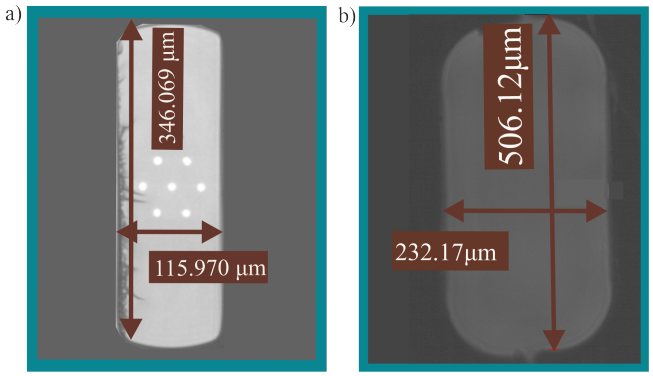

Figure 3: a) Cross-section of the flat fibre. b) Rectangular split dies

Figure 3 shows the cross-section of the flat fibre as well as the dimensions of the custom-made gravity fed rectangular split-dies that were used for coating the flat fibre.

For the flat fibre draw, the furnace was operated at around 1830°, a temperature lower than the common draw temperature (2000°) that is necessary to avoid the circularisation of the fibre. The fibre was pulled with a tension of 160 g at a speed of 10.1 m/min. The feed rate was 1.1 mm/min. It is also important to avoid any twist of the fibre during the draw since this will cause a frozen-in twist within the fibre. Figure 2 shows the geometry of the multi-core fibre that was used as the sensing element. The fibre has a pitch of 35 μm and a core diameter of 5.3 μm.

3.3. Experimental Procedure

For demonstrating the twist elimination a Brillouin Gain Spectrum (BGS) from the flat fibre was acquired. 94 m of the flat 7CF were wrapped in a 150 mm spool. One end of the fibre was spliced to a 7CF flat fibre fan-out and the other end was left free. The splice was performed using a Fujikura 100P+ splicer with a splicing recipe that was optimised for this type of splice. The frequencies of the YIG synthesiser were scanned through a 300 MHz frequency range at 3 MHz steps using an Arduino controller. The selected YIG frequency determined the Brillouin beat frequency that was measured: i.e. the measured component of

the Brillouin spectrum was equal to the YIG frequency plus 1 GHz (the IF). The signal was fed to a storage oscilloscope with a sampling rate of 5 Gs/s, which was used to average 10,000 time-domain traces that were then transferred to the PC. The Brillouin spectrum was built by collecting such traces over a range of frequencies determined by the YIG synthesizer [14]. The processes of scanning the frequencies, capturing the data and building the Brillouin gain spectra were automated using a Python script. The automation reduces the time needed for a complete measurement and hence eliminates the introduction of errors due to temperature variations or drift of the electronic equipment.

4. Experimental Results and Discussion

Fig. 4 shows a Brillouin Gain Spectrum (2D and 3D representation) corresponding to an outer core of the flat 7CF. The spectrum has been taken by scanning along a 300 MHz range in 5 MHz step. 10,000 averages were performed at each step.

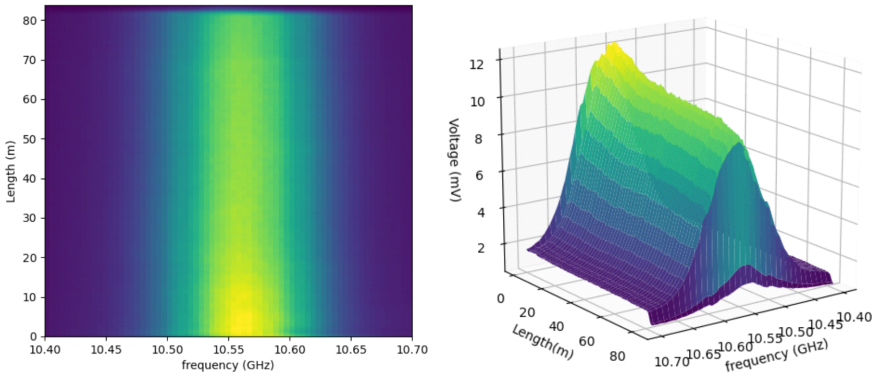

Figure 4: BGS of an outer core for the case of a flat fibre.

For comparison, Fig. 5 shows the BGS for an outer core for the case of a standard circular 7CF, a D-shaped 7CF and the newly designed flat 7CF

wrapped around a spool. The horizontal and vertical axes of this diagram represent the distance along the sensing fibre and the frequency, respectively. All the diagrams were obtained by scanning the BGS over a frequency range of 300 MHz in 5 MHz steps. At each step, the backscattered traces were averaged $10,000$ times to improve the Signal to Noise Ratio (SNR). The difference in the central frequency is due to the fact that the fibre is wrapped around spools of different diameter causing difference in the strain levels experienced by the cores. It is noted that the BGS of a standard 7CF presents notable fluctuations that reflect the random flips of the fibre as it is wrapped around the bobbin. In the case of the D-shaped 7CF there are fewer fluctuations within a 50 m length and it can be clearly seen that the D -shaped fibre flips between two states (either the flat side sits on the inner side of the spool or on the outside). Finally, the flat 7CF shows no visible fluctuations proving that its asymmetric design enhances the preferential bending, rendering it a promising candidate for long range curvature sensing.

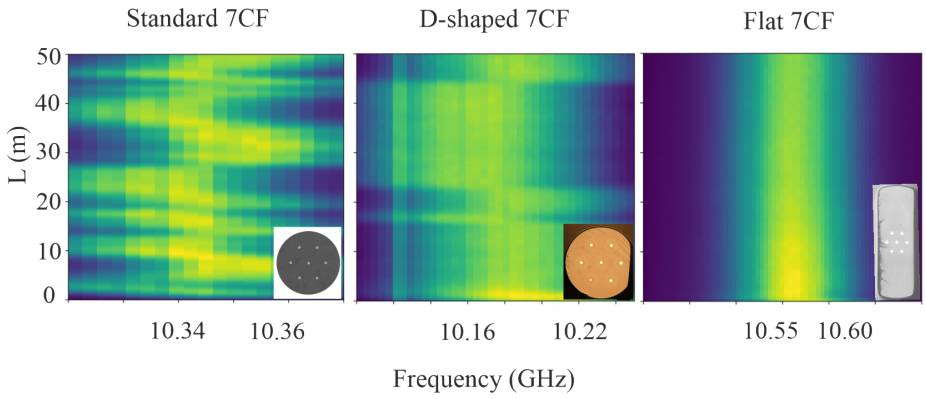

Figure 5: BGS of an outer core for the case of a standard, D-shaped and flat fibre. The spectrum corresponding to the flat 7CF presents no fluctuations reflecting the elimination of twist along the length of the fibre.

5. Conclusion

A multi-core fibre of unique geometry has been designed, fabricated and characterised using a fully distributed Brillouin OTDR setup. Compared to a standard 7CF and a D-shaped fibre, the flat 7CF presents an enhanced preference in bending something that is reflected to its BGS that shows no fluctuations for a length of more than 50 m. This renders the flat multi-core fibre a promising candidate for the field of shape sensing.

6. Funding

This project has received funding from the European Union's Horizon 2020 research and innovation programme under the Marie Sklodowska-Curie grant agreement FINESSE No 722509, from UKRI under grants EP/S013776; NE/S012877/1, and from the Royal Society under the grant CHL\R1 \180350.

References

[1] D. J. Richardson, J. M. Fini, L. E. Nelson, Space-division multiplexing in optical fibres, Nature Photonics 7 (5) (2013) 354–362. doi:10.1038/nphoton.2013.94.
URL http://www.nature.com/articles/nphoton.2013.94

[2] G. M. H. Flockhart, W. N. MacPherson, J. S. Barton, J. D. C. Jones, L. Zhang, I. Bennion, Two-axis bend measurement with bragg gratings in multicore optical fiber, Opt. Lett. 28 (6) (2003) 387–389. doi:10.1364/OL.28.000387.
URL http://ol.osa.org/abstract.cfm?URI=ol-28-6-387

[3] D. Barrera, I. Gasulla, S. Sales, Multipoint two-dimensional curvature optical fiber sensor based on a nontwisted homogeneous four-core fiber, J. Lightwave Technol. 33 (12) (2015) 2445–2450.
URL http://jlt.osa.org/abstract.cfm?URI=jlt-33-12-2445

[4] H. Zhang, Z. Wu, P. P. Shum, R. Wang, X. Q. Dinh, S. Fu, W. Tong, M. Tang, Fiber bragg gratings in heterogeneous multicore fiber for directional bending sensing, Journal of Optics 18 (8) (2016) 085705. doi:10.1088/2040-8978/18/8/085705.
URL https://doi.org/10.1088/2040-8978/18/8/085705

[5] A. Fender, W. N. MacPherson, R. R. J. Maier, J. S. Barton, D. S. George, R. I. Howden, G. W. Smith, B. J. S. Jones, S. McCulloch, X. Chen, R. Suo, L. Zhang, I. Bennion, Two-axis temperature-insensitive accelerometer based on multicore fiber bragg gratings, IEEE Sensors Journal 8 (7) (2008) 1292–1298. doi:10.1109/JSEN.2008.926878.

[6] R. G. Duncan, M. E. Froggatt, S. T. Kreger, R. J. Seeley, D. K. Gifford, A. K. Sang, M. S. Wolfe, High-accuracy fiber-optic shape sensing, San Diego, California, 2007, p. 65301S. doi:10.1117/12.720914.
URL http://proceedings.spiedigitallibrary.org/proceeding.aspx?doi=10.1117/12.720914

[7] E. H. Templeton, D. Kominsky, T. Brown, I. Nesnas, A Novel Sensing Tether for Rovers. arXiv:https://arc.aiaa.org/doi/pdf/10.2514/6.2018-1534, doi:10.2514/6.2018-1534.
URL https://arc.aiaa.org/doi/abs/10.2514/6.2018-1534

[8] Y. Dang, Z. Zhao, M. Tang, C. Zhao, L. Gan, S. Fu, T. Liu, W. Tong, P. P. Shum, D. Liu, Towards large dynamic range and ultrahigh measurement resolution in distributed fiber sensing based on multicore fiber, Opt. Express 25 (17) (2017) 20183–20193. doi:10.1364/OE.25.020183.
URL http://www.opticsexpress.org/abstract.cfm?URI=oe-25-17-20183

[9] G. A. Miller, C. G. Askins, E. J. Friebele, Shape sensing using distributed fiber optic strain measurements, Santander, Spain, 2004, p. 528. doi:10.1117/12.566653.

URL http://proceedings.spiedigitallibrary.org/proceeding.aspx?doi=10.1117/12.566653

[10] Z. Zhao, M. A. Soto, M. Tang, L. Thévenaz, Distributed shape sensing using brillouin scattering in multi-core fibers, Opt. Express 24 (22) (2016) 25211–25223. doi:10.1364/OE.24.025211.
URL http://www.opticsexpress.org/abstract.cfm?URI=oe-24-22-25211

[11] I. Floris, J. M. Adam, P. A. Calderón, S. Sales, Fiber optic shape sensors: A comprehensive review, Optics and Lasers in Engineering 139 (2021) 106508. doi:https://doi.org/10.1016/j.optlaseng.2020.106508.
URL https://www.sciencedirect.com/science/article/pii/S0143816620319461

[12] C. G. Askins, G. A. Miller, E. J. Friebele, Bend and twist sensing in a multiple-core optical fiber, in: OFC/NFOEC 2008 - 2008 Conference on Optical Fiber Communication/National Fiber Optic Engineers Conference, 2008, pp. 1–3. doi:10.1109/OFC.2008.4528404.

[13] P. S. Westbrook, K. S. Feder, T. Kremp, T. F. Taunay, E. Monberg, J. Kelliher, R. Ortiz, K. Bradley, K. S. Abedin, D. Au, G. Puc, Integrated optical fiber shape sensor modules based on twisted multicore fiber grating arrays, San Francisco, California, United States, 2014, p. 89380H. doi:10.1117/12.2041775.
URL http://proceedings.spiedigitallibrary.org/proceeding.aspx?doi=10.1117/12.2041775

[14] I. Floris, J. Madrigal, S. Sales, P. A. Calderón, J. M. Adam, Twisting measurement and compensation of optical shape sensor based on spun multicore fiber, Mechanical Systems and Signal Processing 140 (2020) 106700. doi:https://doi.org/10.1016/j.ymssp.2020.106700.
URL https://www.sciencedirect.com/science/article/pii/S0888327020300868

[15] V. Modes, T. Ortmaier, J. Burgner-Kahrs, Shape sensing based on longitudinal strain measurements considering elongation, bending, and twisting, IEEE Sensors Journal 21 (5) (2021) 6712–6723. doi:10.1109/JSEN.2020.3043999.

[16] L. J. Cooper, A. S. Webb, A. Gillooly, M. Hill, T. Read, P. Maton, J. Hankey, A. Bergonzo, Design and performance of multicore fiber optimized towards communications and sensing applications, in: S. Jiang, M. J. F. Digonnet (Eds.), Optical Components and Materials XII, Vol. 9359, International Society for Optics and Photonics, SPIE, 2015, pp. 82 – 88. doi:10.1117/12.2076950.
URL https://doi.org/10.1117/12.2076950

[17] A. Zafeiropoulou, A. Masoudi, A. Zdagkas, L. Cooper, G. Brambilla, Curvature sensing with a d-shaped multicore fibre and brillouin optical time-domain reflectometry, Opt. Express 28 (2) (2020) 1291–1299. doi:10.1364/OE.383096.
URL http://www.opticsexpress.org/abstract.cfm?URI=oe-28-2-1291

[18] T. Horiguchi, K. Shimizu, T. Kurashima, M. Tateda, Y. Koyamada, Development of a distributed sensing technique using brillouin scattering, Journal of Lightwave Technology 13 (7) (1995) 1296–1302. doi:10.1109/50.400684.

[19] P. Wait, T. Newson, Landau placzek ratio applied to distributed fibre sensing, Optics Communications 122 (4) (1996) 141–146. doi:https://doi.org/10.1016/0030-4018(95)00557-9.
URL https://www.sciencedirect.com/science/article/pii/0030401895005579

[20] C. Galíndez, J. López-Higuera, Brillouin distributed fiber sensors: An overview and applications, Journal of Sensors 2012. doi:10.1155/2012/204121.

[21] J. P. Moore, M. D. Rogge, Shape sensing using multi-core fiber optic cable and parametric curve solutions, Opt. Express 20 (3) (2012) 2967–2973. doi:10.1364/OE.20.002967.
URL http://www.opticsexpress.org/abstract.cfm?URI=oe-20-3-2967

[22] F. Khan, A. Denasi, D. Barrera, J. Madrigal, S. Sales, S. Misra, Multi-core optical fibers with bragg gratings as shape sensor for flexible medical instruments, IEEE Sensors Journal 19 (14) (2019) 5878–5884. doi:10.1109/JSEN.2019.2905010.

[23] A. Masoudi, T. P. Newson, Contributed review: Distributed optical fibre dynamic strain sensing, Review of Scientific Instruments 87 (1) (2016) 011501. arXiv:https://doi.org/10.1063/1.4939482, doi:10.1063/1.4939482.
URL https://doi.org/10.1063/1.4939482

[24] V. I. Kopp, J. Park, M. Wlodawski, J. Singer, D. Neugroschl, A. Z. Genack, Chiral fibers: Microformed optical waveguides for polarization control, sensing, coupling, amplification, and switching, Journal of Lightwave Technology 32 (4) (2014) 605–613. doi:10.1109/JLT.2013.2283495.

[25] M. N. Alahbabi, N. P. Lawrence, Y. T. Cho, T. P. Newson, High spatial resolution microwave detection system for brillouin-based distributed temperature and strain sensors, Measurement Science and Technology 15 (8) (2004) 1539–1543. doi:10.1088/0957-0233/15/8/019.
URL https://doi.org/10.1088/0957-0233/15/8/019

[26] J. Yamamoto, T. Yajima, Y. Kinoshita, F. Ishii, M. Yoshida, T. Hirooka, M. Nakazawa, Fabrication of multi core fiber by using slurry casting method, in: Optical Fiber Communication Conference, Optical Society of America, 2017, p. Th1H.5. doi:10.1364/OFC.2017.Th1H.5.
URL http://www.osapublishing.org/abstract.cfm?URI=OFC-2017-Th1H.5

[27] S. R. Nagel, J. B. MacChesney, K. L. Walker, An overview of the modified chemical vapor deposition (mcvd) process and performance, IEEE Transactions on Microwave Theory and Techniques 30 (4) (1982) 305–322. doi:10.1109/TMTT.1982.1131071.